EFFECT OF PREPLASMAS ON HIGH-ENERGY ION GENERATION BY AN INTENSE LASER PULSE IRRADIATED ON OVERDENSE PLASMAS

Hae June Lee * Jincheol B. Kim, Changbum Kim, Guang-Hoon Kim, Jong-Uk Kim, Hyyong Suk,
Korea Electrotechnology Research Institute, Changwon, 641-120, Republic of Korea

Abstract

High-energy ion generation from the interaction of an ultrashort intense laser pulse with an overdense plasma slab is studied with fully electromagnetic and relativistic particle-in-cell simulation. With a properly designed underdense preplasma, we observed that the forward ion acceleration from the front surface can be enhanced. The momentum distribution functions of the accelerated ions are investigated with respect to the laser pulse intensity and the preplasma profile.

INTRODUCTION

With the fast development of laser technology, the relativistic interaction of a super intense laser pulse with plasmas attracted lots of interests in the society of particle accelerators. Advanced acceleration concepts using a laser pulse can be applied for the generation of ions [1, 2, 3, 4] as well as electrons [5, 6, 7] due to the enhancement in the intensity and the pulse duration with the help of chirped pulse amplification (CPA) technique.

Two mechanisms of forward ion acceleration from a solid target irradiated by an ultrashort intense laser pulse were introduced recently. One is the ion generation from the rear surface [1, 2], and the other is that from the front surface [3, 4]. The former is generated by hot electrons penetrating through the slab and has low emittance and high maximum energy. However, the energy spread of the accelerated ions is large. The latter is produced by a shock wave produced by the ponderomotive force of the laser pulse and has low energy spread. It was also reported that the advantages of both of them can be combined as the ions initially formed in the shock wave at the front surface reach the rear side of the exploding plasma layer and are further accelerated by the electric field produced by the hot electrons [8].

In this study, we investigate the effect of preplasmas on the formation of the ion shock wave in the front surface by using one-dimensional (1d) electromagnetic particle-in-cell (PIC) code (1D-XOOPIC) [9] and two-dimensional (2d) one (OSIRIS) [10] in order to achieve high maximal ion energy.

* E-mail address : leehj@keri.re.kr. This work is supported by the Creative Research Initiatives of the Korea Ministry of Science and Technology.

SIMULATION PARAMETERS

For 1d simulation, we use a linearly polarized plane wave with a Gaussian profile,

$$E_z(x,t) = E_0 \exp[-(x-x_c)^2/c^2\tau_L^2]\sin(kx-\omega_0 t), \quad (1)$$

where E_z is the transverse electric field, E_0 is the maximum electric field, $x_c(t)$ is the center position of the laser pulse, ω_0 is the frequency, k is the wavenumber, and τ_L is the pulse duration of the laser pulse. The wavelength in vacuum is set to $\lambda_0 = 2\pi/k = 1\ \mu$m and the full width at half maximum (FWHM) is calculated as 1.18 $c\tau_L$, where c is the speed of light. For 2d simulation, the laser pulse is linearly polarized and has a Gaussian profile also in the transverse direction.

The laser intensity is represented as a normalized vector potential,

$$a = \frac{eE_0}{mc\omega_0}, \quad (2)$$

which can be expressed with the laser intensity (I) as

$$a = 0.85 \times 10^{-9}\lambda_0\sqrt{I}. \quad (3)$$

Here, I is in W/cm^2 and λ_0 is in μm. The target is assumed to be a fully ionized cold plasma slab with thickness of 2 μm composed of protons and electrons with density of n_e. Mainly $n_e = 10^{23}$ cm^{-3} $= 90\ n_c$ is used in the simulation, where n_c is the critical density of the laser pulse. The electron plasma frequency for this case is, $\omega_p = (n_e e^2/\epsilon_0 m)^{1/2}$, which is about ten times larger than the laser frequency, ω_0. Here, e, ϵ_0, and m are the elementary charge, the vacuum permittivity, and the electron mass, respectively.

For 1d simulation, The simulation domain was set to have a length of 100 μm and the target is located at x_0 = 50 μm. A laser pulse is launched from the left side of the simulation domain at $t = 0$ and propagates toward the target. The grid size is $\Delta x = 3.9$ nm (256 cells per one wavelength) and the time step is $\Delta t = 0.0065$ fs ($\Delta x/\Delta t = 2c$). Note that $\omega_p \Delta t \approx 0.12 < 1.0$, which is small enough to simulate the electron motions in the overdense plasma regime.

For 2d simulation, however, simulation time becomes very long to calculate with the same size of simulation domain as that of 1d case. Therefore, we simulated the case of $n_e = 10^{22}$ cm^{-3} $= 9\ n_c$ instead of $n_e = 10^{23}$ cm^{-3} just in order to confirm that the tendency of 1d and 2d simulation results are almost similar. The grid size is $\Delta x = 31.3$ nm (32 cells per one wavelength), and the time step is $\Delta t = 0.076$ fs ($\Delta x/\Delta t = 1.38c$) for 2d simulation. In this case, $\omega_p \Delta t \approx 0.44 < 1.0$. For a higher plasma density, the grid size should be reduced.

In order to represent wide density ranges of the preplasma, we used varying ratios of the simulation particles to real particles. Because of small collision cross sections for fast moving particles, the collisions of electrons and ions with neutrals are neglected.

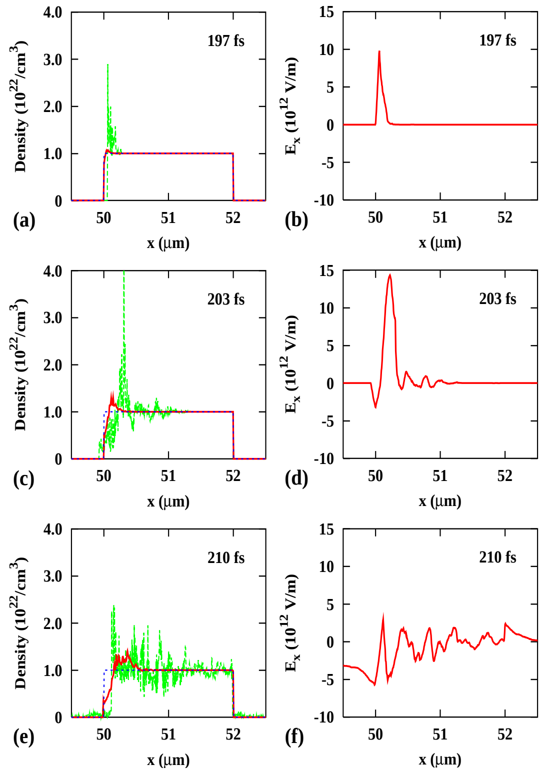

Figure 1: Shown are the profiles of the ion (solid) and electron (dashed) densities [(a), (c), and (e)] and the longitudinal electric field [(b), (d), and (f)] at different time. The dotted line in the density profiles shows the initial plasma profile. Simulation parameters are $a = 10$, $\tau_L = 10$ fs, and $n_e = 9\, n_c$.

RESULTS

Figure 1 shows the evolution of plasma density and longitudinal electric field in 1d simulation. When the laser pulse has been incident on the plasma slab, electrons are pushed by the ponderomotive force of the intense laser pulse and the charge separation produces strong longitudinal electric field as shown in Figs. 1(a) and 1(b). Due to the strong electric field, ions begin to move, and some electrons are pulled backward while hot electrons propagates inside the slab as shown in Figs. 1(c) and 1(d). Even after the laser pulse has been reflected back, the hot electrons penetrate through the plasma slab and make strong electric field also in the rear side. Finally, there are three types of ion acceleration which are the backward ion acceleration (BIA) at the front side, the forward ion acceleration at the rear side (FIAR), and the forward ion acceleration at the front side (FIAF) [8]. As shown in Fig. 1(e), the ion density in FIAF is high, and thus it is possible to increase the total amount of charges of the ion beam if we can utilize FIAF properly.

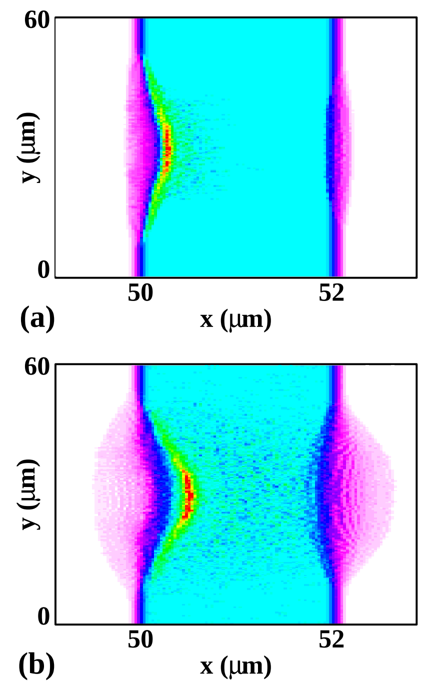

Figure 2: Density profile of the ions at (a) $t = 239$ fs and (b) $t = 292$ fs. Simulation parameters are $a = 5$, $\tau_L = 10$ fs, and $n_e = 9\, n_c$.

With the same parameters, we observed that the 2d simulation results at the center plane of the Gaussian laser pulse agree qualitatively well with those shown in Fig. 1. Figure 2 shows the 2d ion density profiles at later time far after the laser pulse has been reflected. BIA, FIAR, and FIAF are clearly recognized in Fig. 2(b).

We investigated the effect of underdense preplasmas which can be generated by a prepulse. The preplasma is formed in front of the target and assumed to have an exponential density profile, $n(x) = n_1 e^{\kappa(x-x_0)}$, over range of 10 μm. Here, n_1 is the maximum density of the preplasma, x_0 is the location of the plasma slab, and κ is the scale factor of the preplasma profile. In the simulations, we set κ to be 0.69 μm^{-1}, and varied n_1 from $10^{-3} n_c$ to $0.9\, n_c$. Note that the collisionless skin depth is $\delta \approx c/\omega_p = 0.0168$ μm for $n_e = 10^{23}$ cm^{-3}, which is much shorter than the target thickness of 2 μm.

Figure 3 shows the enhancement of the ion acceleration at the front surface with the maximum preplasma density close to the critical density, n_c. The maximum value of the ion momentum in the longitudinal direction, P_x, does not change much when n_1 is small, but it increases more than 30% when $n_1 = 0.9 n_c$ compared with the case without the preplasma. The enhancement is caused by the electrons

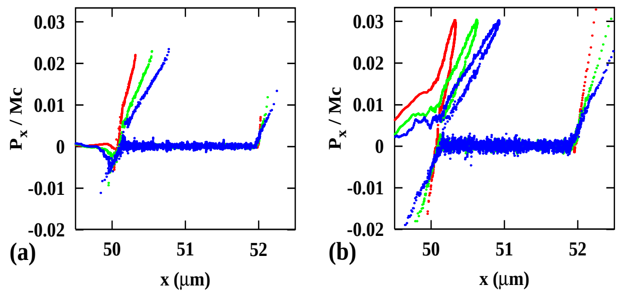

Figure 3: Momentum-position phase space for the cases of (a) $n_1 = 10^{-3}n_c$ and (b) $n_1 = 0.9n_c$ at $t = 253$ fs, 287 fs, and 320 fs. Simulation parameters are $a = 5$, $\tau_L = 10$ fs.

which is accelerated from the preplasma and penetrate into the plasma slab. They produces more strong longitudinal electric field at the front surface where the laser pulse is reflected. It was observed that not only the maximum energy of FIAF but also that of FIAR increases with the preplasma.

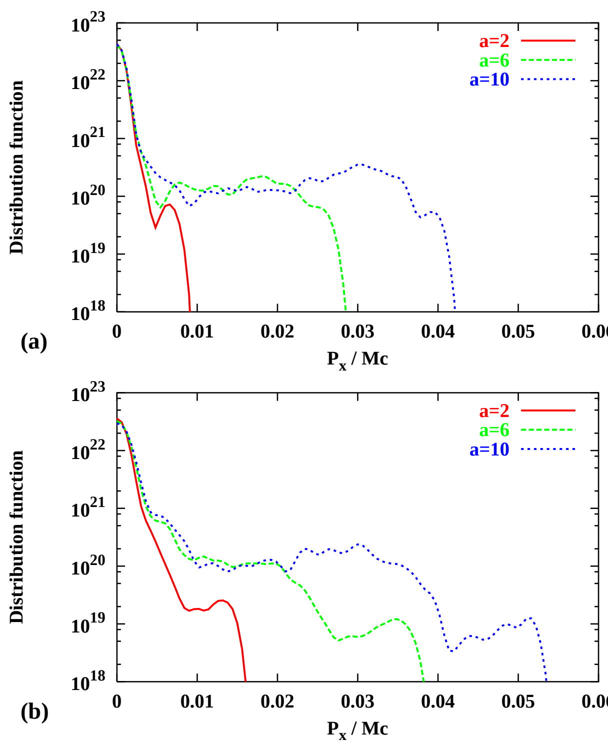

Figure 4: Momentum distribution functions of the accelerated ions for different laser intensities (a) without preplasmas and (b) with an exponential-profiled preplasma for $n_1 = 0.9n_c$. The profiles are measured at $t = 247$ fs.

Figure 4 shows the comparison of the momentum distribution function with and without preplasmas. For both the cases, the maximal ion momentum increases as the laser intensity increases. Here, a is proportional to $I^{1/2}$ with the relation of Eq. (3). As shown in Fig. 4(b), the distribution functions have a high energy tail and thus the maximal ion momentum increases when there is a preplasma with a proper density profile.

CONCLUSION

We simulated high-energy ion generation from the interaction of ultrashort intense laser pulse with an overdense plasma slab which has exponential-profiled preplasmas. The forward ion acceleration from the front surface with the formation of an ion shock wave is investigated. The one-dimensional and the two-dimensional simulation results show the same tendency for the profile evolution of the plasma density and the induced longitudinal electric field. With a preplasma of which maximum density is close to the critical density of the laser pulse, the accelerated ion energy has been enhanced more than 30% compared with the case without preplasma.

REFERENCES

[1] S. P. Hatchett *et al.*, Phys. Plasmas **7**, 2076 (2000).

[2] Y. Murakami *et al.*, Phys. Plasmas **8**, 4138 (2001).

[3] A. Maksimchuk *et al.*, Phys. Rev. Lett. **84**, 4108 (2000).

[4] T. Zh. Esirkepov *et al.*, JETP Lett. **70**, 82 (1999).

[5] T. Tajima and J. M. Dawson, Phys. Rev. Lett. **43**, 267 (1979).

[6] M. Everett, A. Lal, D. Gordon, C. E. Clayton, K. A. Marsh, and C. Joshi, Nature **368**, 527 (1994).

[7] K. Nakajima *et al.*, Phys. Rev. Lett. **74**, 4428 (1995).

[8] A. Zhidkov *et al.* Phys. Rev. Lett. **89**, 215002, (2002).

[9] J. P. Verboncoeur, A. B. Langdon, and N. T. Gladd, Comp. Phys. Comm., **87**, 199 (1995); H. J. Lee, P. J. Mardahl, G. Penn, and J. S. Wurtele, IEEE Trans. Plasma Science **30**, 40 (2002).

[10] R. G. Hember *et al.*, Phys. Rev. E **57**, 5920 (1998).